Accepted Manuscript

Synthesis and biological evaluation of vanadium complexes as novel anti-tumor agents

Ling-Pan Lu, Feng-Zhi Suo, Ya-Li Feng, Li-Li Song, Ying Li, Yang-Jie Li, Kai-Ti Wang

PII: S0223-5234(19)30401-5

DOI: https://doi.org/10.1016/j.ejmech.2019.04.073

Reference: EJMECH 11308

To appear in: *European Journal of Medicinal Chemistry*

Received Date: 30 December 2018

Revised Date: 17 April 2019

Accepted Date: 29 April 2019

Please cite this article as: L.-P. Lu, F.-Z. Suo, Y.-L. Feng, L.-L. Song, Y. Li, Y.-J. Li, K.-T. Wang, Synthesis and biological evaluation of vanadium complexes as novel anti-tumor agents, *European Journal of Medicinal Chemistry* (2019), doi: https://doi.org/10.1016/j.ejmech.2019.04.073.

Graphic abstract

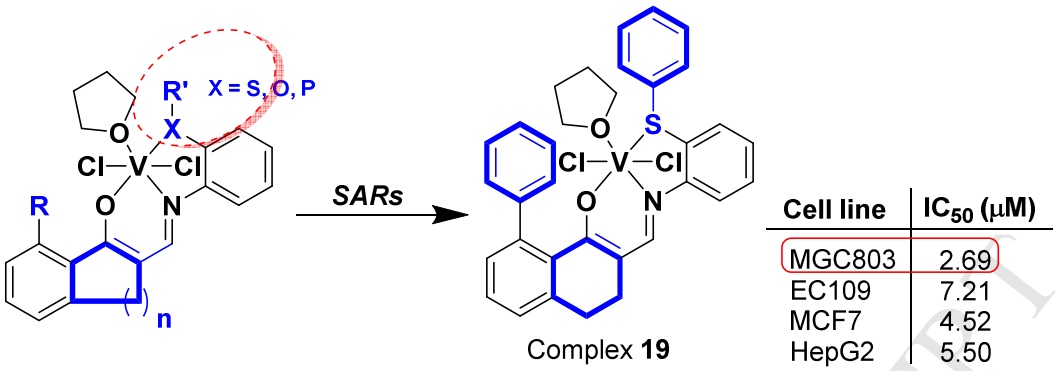

Complex **19**

Cell line	IC_{50} (μM)
MGC803	2.69
EC109	7.21
MCF7	4.52
HepG2	5.50

Synthesis and biological evaluation of vanadium complexes as novel anti-tumor agents

Ling-Pan Lu [a], Feng-Zhi Suo [c], Ya-Li Feng [a], Li-Li Song [a], Ying Li [d], Yang-Jie Li [a], Kai-Ti Wang [b,*]

[a] *School of Pharmaceutical Sciences, Zhengzhou University of Industrial Technology, Zhengzhou,451199, PR Chin*a

[b] *School of Materials Science and Engineering, Chongqing University of Technology, Chongqing 400054, PR China*

[c] *School of Pharmaceutical Sciences, Zhengzhou University, Zhengzhou 450001, PR China*

[d] *Department of Pharmacy, The First Affiliated Hospital of Zhengzhou University, Zhengzhou 450001, PR China*

[*]Corresponding Author

E-mail address: ktwang@cqut.edu.cn

ABSTRACT: A class of vanadium complexes were prepared and investigated for their antiproliferative effects by MTT assay. The structure-activity relationship was extensively studied through the ligand variation. The results showed that the synthetic vanadium complexes demonstrated moderate to good antiproliferative activities against the four cancer cell lines including MGC803, EC109, MCF7 and HepG2, respectively. Of note was that most of the complexes showed preferential growth inhibitory activity to some degree toward gastric cancer line MGC803. Among them, complex **19** exhibited the most and broad-spectrum proliferative inhibition against the tested cell lines. In addition, mechanism studies illustrated that complex **19** could prevent the colony formation, migration and EMT process, as well as induce apoptosis of MGC803 cells. Furthermore, western blot experiments revealed that the expression of apoptosis-related proteins changed, including up-regulation of Bax, PARP and caspase-3/9, as well as down-regulation of Bcl-2.

Keywords: Vanadium complex; Antiproliferative effects; Migration; Apoptosis

1. INTRODUCTION

Vanadium, an essential and required trace element for human body, plays an important role in biochemical processes [1, 2]. Vanadium complexes possess a broad range of pharmacological properties such as anti-diabetes, anti-parasitism, anti-HIV, anti-tuberculosis and anti-cancer activities [3-7], and therefore spur extensive research interest in medicinal chemistry [5]. With the intensive study of medicinal metallochemsitry, various bioactive vanadium complexes have been increasingly developed. As shown in Fig. 1, vanadyl-hypocrellin **A** complex could not only improve the water solubility of hypocrellin, but also increase its photostability, affinity and anti-cancer activity [8]. In addition, vanadium complexes were widely studied to exhibit insulin-mimetic effects and antidiabetic activities probably by a nonspecific inhibition of phosphotyrosine phosphatase [9, 10]. For example, dioxidovanadium (V) complex **B** was reported as a potent and selective protein tyrosine phosphatase 1B (PTP1B) inhibitor, exhibiting anti-diabetic activity as well as low cytotoxicity in vitro [11]. And vanadyl complex **C** with schiff base as organic ligands could not only reduce the blood glucose level and improve the impaired glucose tolerance in a diabetic rat model, but also show good lipophilic properties and low cytotoxicity on Caco-2 cell line [9]. Moreover, vanadocene dichloride **D** (Fig. 1), characterized by two cyclopentadienyl rings and both chlorine atoms coordinating to the vanadium center in a “bent-sandwich” structure [12], was identified to have antitumor effects on a wide spectrum of cancer cells such as testicular cancer, leukemia, breast cancer, glioblastoma and colon cancer [13-16]. A recent research showed that vanadocene dichloride could selectively inhibit the proliferation of Hela cells over the normal cells, due to the inactivation of serine-threonine protein kinase Aurora B [12]. Moreover, water soluble complex **E**, prepared by coordination of antibiotic cefuroxime with vanadyl sulfate in aqueous solution, was reported to exert manifold effects including antimicrobial activity, non-cytotoxicity and immunosuppressive activity [17].

As a continuation of our works [18], in order to find bioactive vanadium complexes with potent and specific anticancer activities, we herein reported the synthesis of a library of novel vanadium complexes, their antiproliferative activities as well as preliminary mechanisms of inducing cell apoptosis.

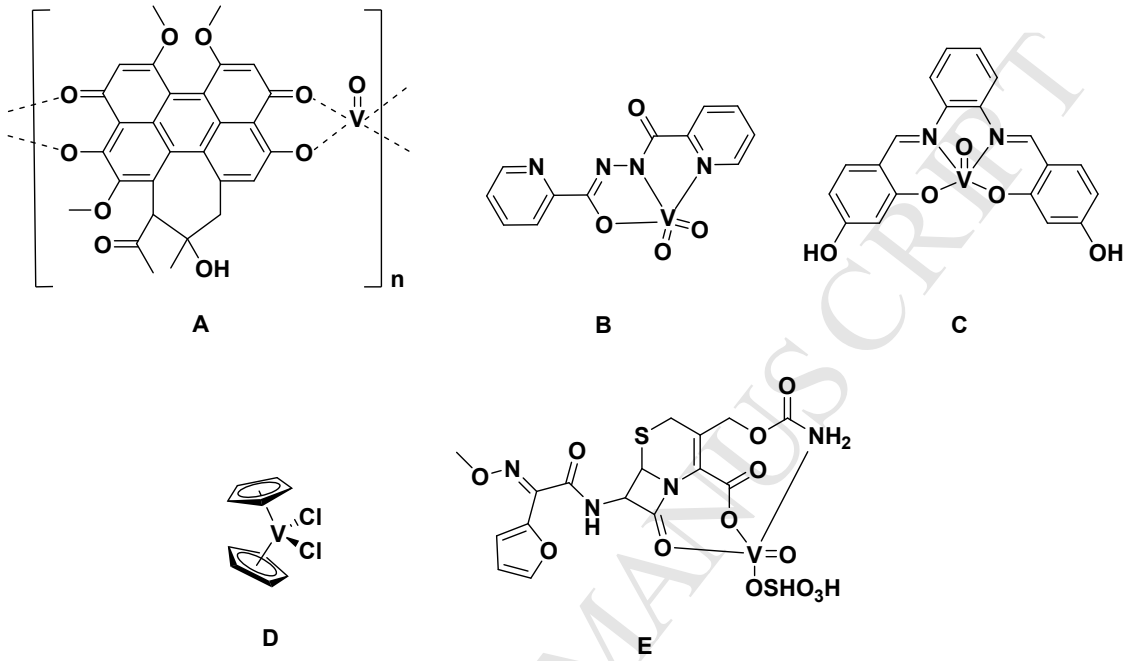

Fig.1. Biologically active vanadium complexes reported.

2. Results and discussion

2.1 Chemistry

The general synthetic route of the targeted complexes is depicted in Scheme 1. The indene derivatives **2a-i** were prepared by reacting indanone analogue **1** and ethyl formate in diethyl ether in the presence of potassium tert-butoxide. 2-(Phenylthio)aniline **3** was prepared by reaction of thiophenol with 2-iodoaniline catalyzed by a combination of cuprous chloride with cyclohexane-1,2-diamine in water [19]. For the synthesis of 2-phenoxyaniline **5**, it was generated by heating iodobenzene, 2-aminophenol and cesium carbonate in the presence copper powder as catalyst [20]. In addition, 2-chloroaniline reacted with triphenylphosphine catalyzed by anhydrous nickel chloride to produce **8**, which was subsequently treated with sodium naphthalenide at low temperature to afford diphenylphosphanyl aniline **9**. And compound **11** was obtained through oxidation of aniline **9** with 30% hydrogen

peroxide. Subsequently, various imine ligands were readily obtained by condensation reaction of the obtained aniline derivatives with indene derivative **2** at room temperature. Finally, the desired vanadium complexes **14-27** were produced by treating ligands with NaH in THF, followed by adding to the solution of $VCl_3(THF)_3$ to proceed coordination reaction (Scheme 2). Additionaly, crystals of complexes **16** and **22** suitable for X-ray cyrstal analysis were grown from the chilled THF and hexane mixture solution, and the data were appended in supporting information (Fig. S1 and Table S1/S2).

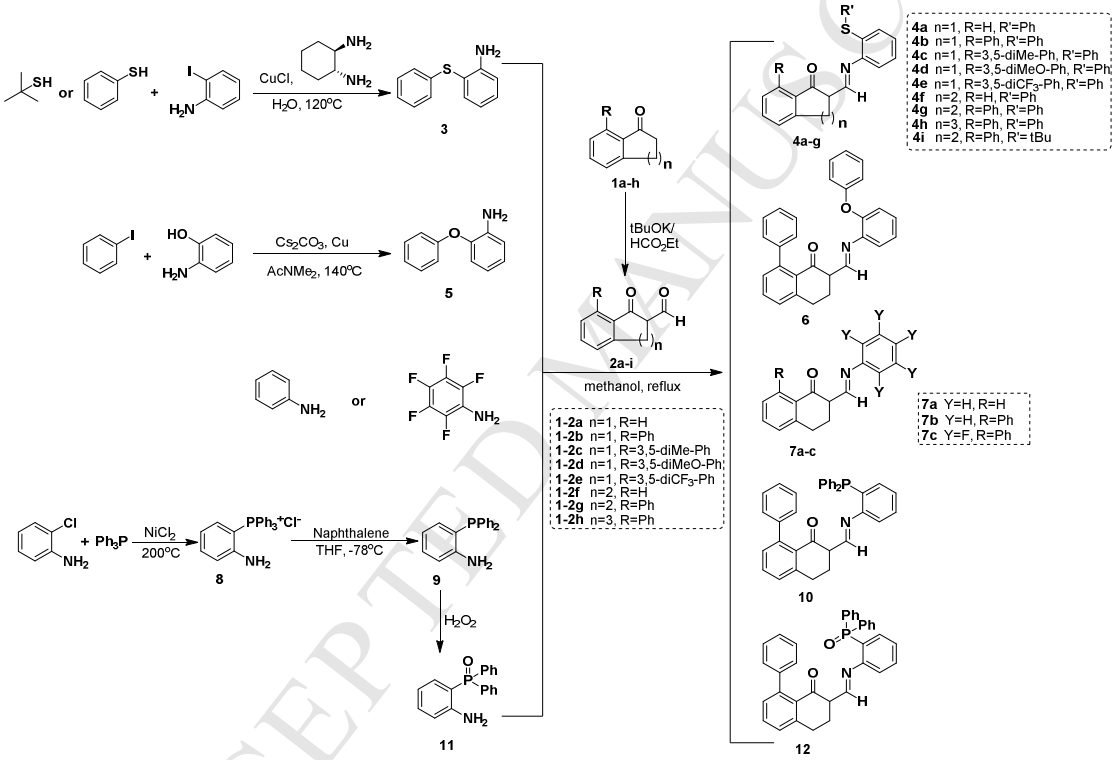

Scheme 1. Synthesis of ligand block.

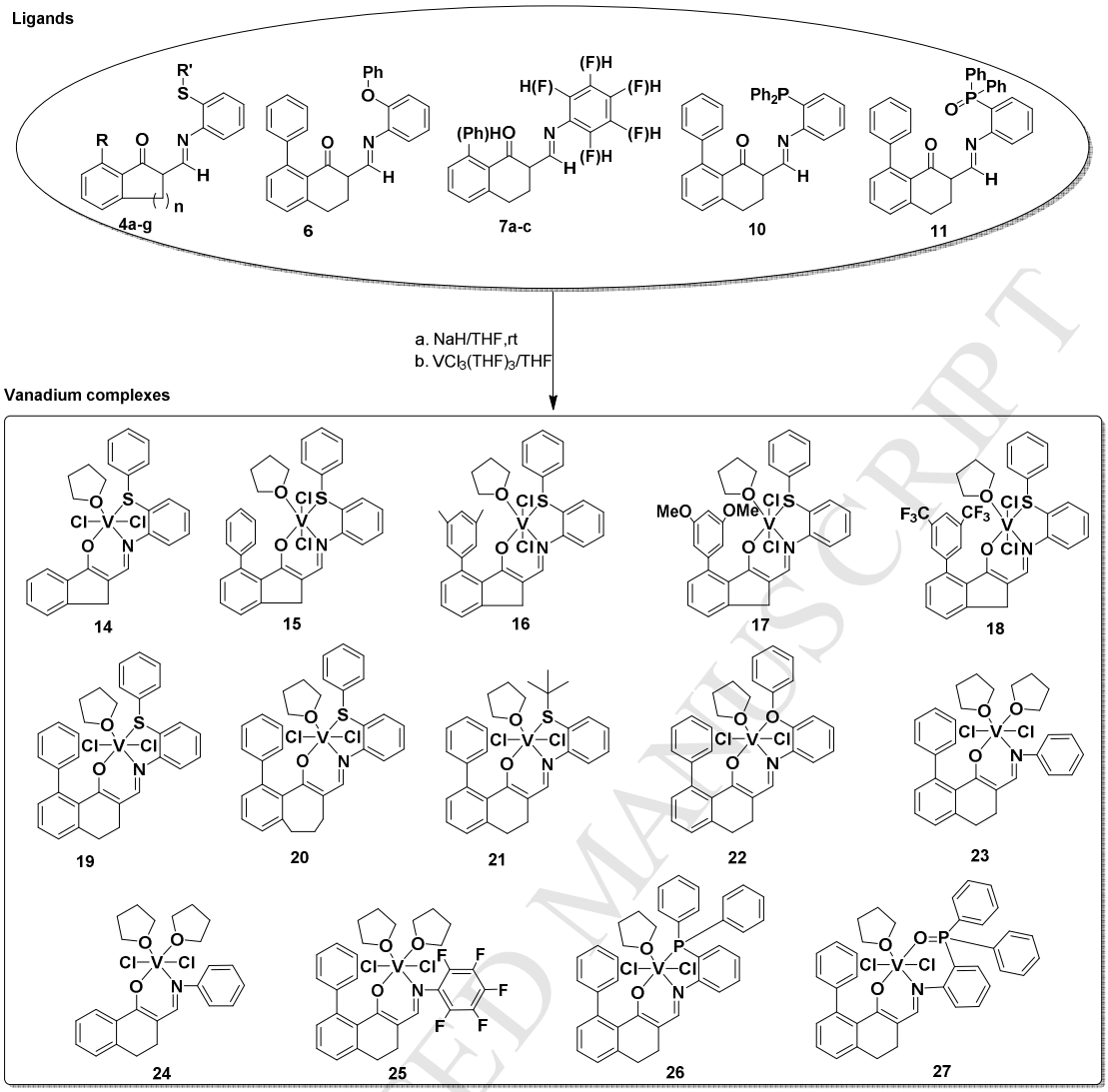

Scheme 2. Synthesis of vanadium complex library.

2.2 Evaluation of biological activity

2.2.1 Antiproliferative activity

Complexes **14-27** were prepared and investigated for their antiproliferative effects on several cancer cell lines including MGC803 (human gastric cancer cell line), EC109 (human esophageal cancer cell line), MCF7 (human breast cancer cell line) and HepG2 (human hepatocellular cancer cell line), by using the MTT assay. The clinical anticancer drug 5-fluorouracil (5-Fu) was employed as the reference drug [21]. Besides, vanadocene dichloride (D) was also evaluated for its inhibitory activity in order to make comparison with the synthetic vanadium complexes in this work. The antiproliferative data are summarized in Tables 1-2.

Initially, complexes **14-21** were screened toward the tested cancer cell lines, with the aim to explore the impact of indannoe structure on the cell proliferation inhibitory ablities. As shown in Table 1, complex **14** showed good and preferred growth inhibition against the gastric cancer cell line MGC803 with single digit IC_{50} value, in comparison to the moderate inhibition against EC109, MCF7 and HepG2 cell lines. And complex **15** with phenyl substitution (R) generally displayed slightly improved antiproliferative activities, compared to that of complex **14** with hydrogen atom substitution. Interestingly, the introduction of 3,5-dimethyl phenyl to R position, generating complex **16**, led to evidently improved cell proliferation inhibition toward all test cancer lines, however, its analogues complex **17** and **18** generally displayed decreased inhibitory activities (IC_{50}s > 32 μM) as well as selective inhibition toward MGC803 cell line (IC_{50} = 7.29 and 15.90 μM, respectively). Intriguingly, the ring expansion from 5- to 6-membered ring of indanone to give complex **19**, exerted significantly improved potent and broad proliferation inhibitory activities against all test cell lines, with IC_{50} values ranging from 2.69 to 7.21 μM. However, 7-membered analogue complex **20** presented sharply decreased inhibitory abilities, in comparison to that of complex **15** and **19**. Furthermore, the replacement of thiophenol fragment with methylpropanethiol (complex **21**) led to a generally decreased activity compared with its counterpart complex **19**. The evaluation of this series of complexes featured by thiolphenol as one of the ligands revealed that the phenyl group for R position and a six-membered ring indanone were favorable to elicit growth inhibition of the test cancer cells, highlighting the structural requirements of this new chemotype metallo compounds for the tumor suppression. Next, complexes **22-25** were produced in order to investigate the effect of additional ligand variations on the antiproliferative activity. As shown in Table 2, complex **22-25** were found to be less active than complex **19**, suggesting that phenol group as ligand part seemed to be disfavored to the activity. It should be noted that complex **22-25** all showed selective inhibitory activities toward MGC803 cell line, consistent with that of aforementioned thiophenol series. Finally, complex **26** and **27** with triphenylphosphine (oxide) as ligand part were prepared and tested for their activities. The results showed that complex **26** was evidently less

active than its oxide analogue complex **27**, indicating the importance of the properties of coordination atom to the vanadium metal center.

Table 1. Antiproliferative activity of complex 1**4-21** against the tested cancer cell lines.

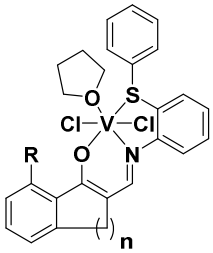

14-20

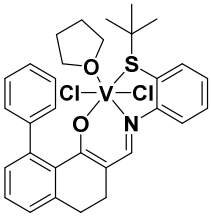

21

Complex	R	n	IC_{50} (μM)[a]			
			MGC803	EC109	MCF7	HepG2
14	H	1	4.79±0.57	16.81±1.19	16.42±1.21	17.96±1.25
15	Ph	1	3.62±0.55	12.29±1.09	12.06±1.08	14.74±1.16
16	3,5-diMe-Ph	1	10.99±1.04	4.00±0.60	2.89±0.46	5.00±0.70
17	3,5-diMeO-Ph	1	7.29±0.86	>32	>32	>32
18	3,5-diCF_3-Ph	1	15.90±1.20	>32	>32	>32
19	Ph	2	2.69±0.56	7.21±0.85	4.52±0.65	5.50±0.74
20	Ph	3	6.48±0.81	13.04±1.11	>32	>32
21	-	-	4.48±0.65	9.00±0.95	7.22±0.85	11.24±1.05
D	-	-	>32	>32	>32	>32
5-Fu	-	-	6.92±0.88	7.15±1.25	9.08±0.94	11.21±1.54

[a]Inhibitory activity was assayed by exposure for 72 h to substance and expressed as concentration required to inhibit tumor cell proliferation by 50% (IC_{50}). Data are presented as the means ± SDs of three independent experiments.

Table 2. Antiproliferative activity of complex **22-27** against the tested cancer cell lines.

No.	Structure	IC_{50} (μM)[a]			
		MGC803	EC109	MCF7	HepG2

22	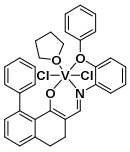	6.24±0.79	19.16±1.28	>32	22.92±1.36
23	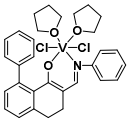	9.42±0.97	10.50±1.02	9.77±0.99	>32
24	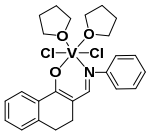	5.07±0.70	11.11±1.04	8.05±0.90	9.53±0.97
25	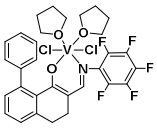	4.95±0.69	>32	>32	>32
26	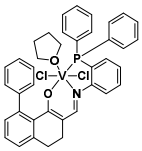	15.74±1.19	14.21±1.15	13.16±1.11	>32
27	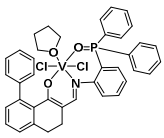	3.13±0.50	8.33±0.72	7.35±0.86	6.50±1.08
D	-	>32	>32	>32	>32
5-Fu	-	6.92±0.88	7.15±1.25	9.08±0.94	11.21±1.54

[a] Inhibitory activity was assayed by exposure for 72 h to substance and expressed as concentration required to inhibit tumor cell proliferation by 50% (IC_{50}). Data are presented as the means ± SDs of three independent experiments.

2.2.2 Cell clonogenicity and migration

The most active as well as broad-spectrum proliferative inhibition of complex **19** spurred us to have an preliminary understanding of its effect on cell colony formation inhibition. This assay measured the ability of tumor cells to grow and form foci in a way that was not restricted by growth contact inhibition, which was characteristic in normal untransformed cells, and therefore clonogenicity was commonly employed as an indirect evaluation of tumor cells undergoing neoplastic transformation [22, 23]. As shown in Fig. 2A, fewer and smaller colonies cells were observed after treatment of MGC803 with complex **19**, and the colony inhibition rate reached around high 90% at 2 μM. Additionally, the effect of complex **19** on the migration ability of MGC803

cells was also investigated by transwell assay. The results revealed that complex **19** markedly inhibited the migration of MGC803 cells dose-dependently (Fig. 2B). Meanwhile, western blot results showed that the expression of mesenchymal cell marker N-cadherin protein decreased, while epithelial cell biomarker E-cadherin increased, indicating that complex **19** possibly prevented the migration of MGC803 via the inhibition of EMT process (epithelial-mesenchymal transition) (Fig. 3).

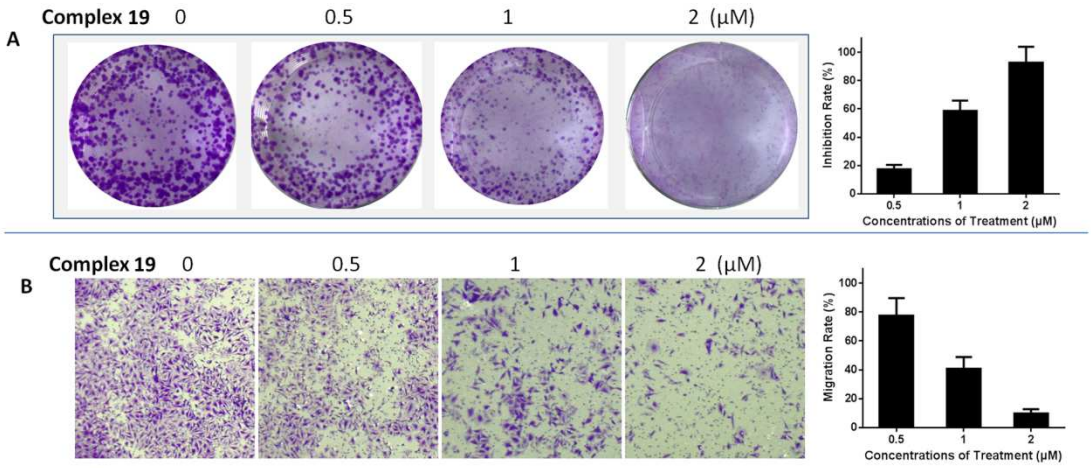

Fig. 2. (A) Representative images of MGC803 cell colonies after treatment with indicated concentrations of complex **19** for 9 d; (B) Migration inhibition of MGC803 by complex **19** at indicated doses via transwell assay. The results shown were representative of three independent experiments.

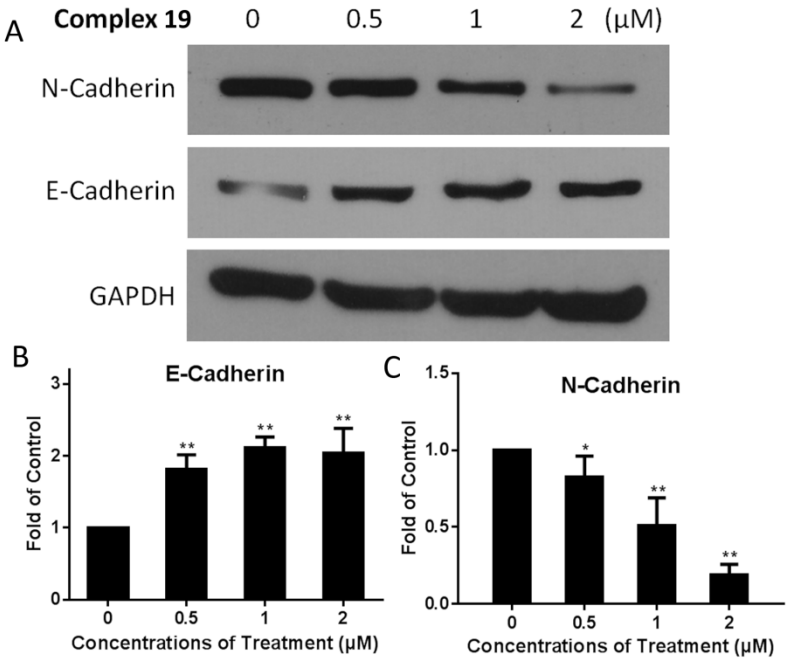

Fig. 3. Expression of E-Cadherin and N-Cadherin when cells were treated with complex **19** at indicated concentrations. **P<0.01 was considered statistically highly significant. Data are mean ± SD. All experiments were carried out at least three times.

2.2.3 Cell apoptosis and mechanism involved

Next, complex **19** was assessed for its ability to induce apoptosis of MGC803 cells. Cell apoptosis is also known as programmed cell death, accompanying characteristic morphological changes and specific biochemical features [24]. Initially, the Hochest 33258 staining was performed to examine the cell morphological changes [25]. Over a period of 24 h incubation with complex **19** at indicated concentrations, characteristic cell morphologic changes such as chromatin shrinkage, rounding and formation of apoptotic bodies were observed and presented a dose-response feature (Fig. 4A), suggesting that the apoptosis of MGC803 cells could be induced by complex **19** concentration-dependently. In order to further examine the effect of complex **19** on the apoptosis of MGC803 cells, Annexin V-FITC/PI double staining method was used for the apoptosis analysis. As shown in Fig. 4B, incubation of MGC803 cells with complex **19** led to a dose-dependent apoptosis increase, with the percentage of apoptosis cells of 12.0%, 17.7% and 36.6%, respectively, compared to the control (0.9%).

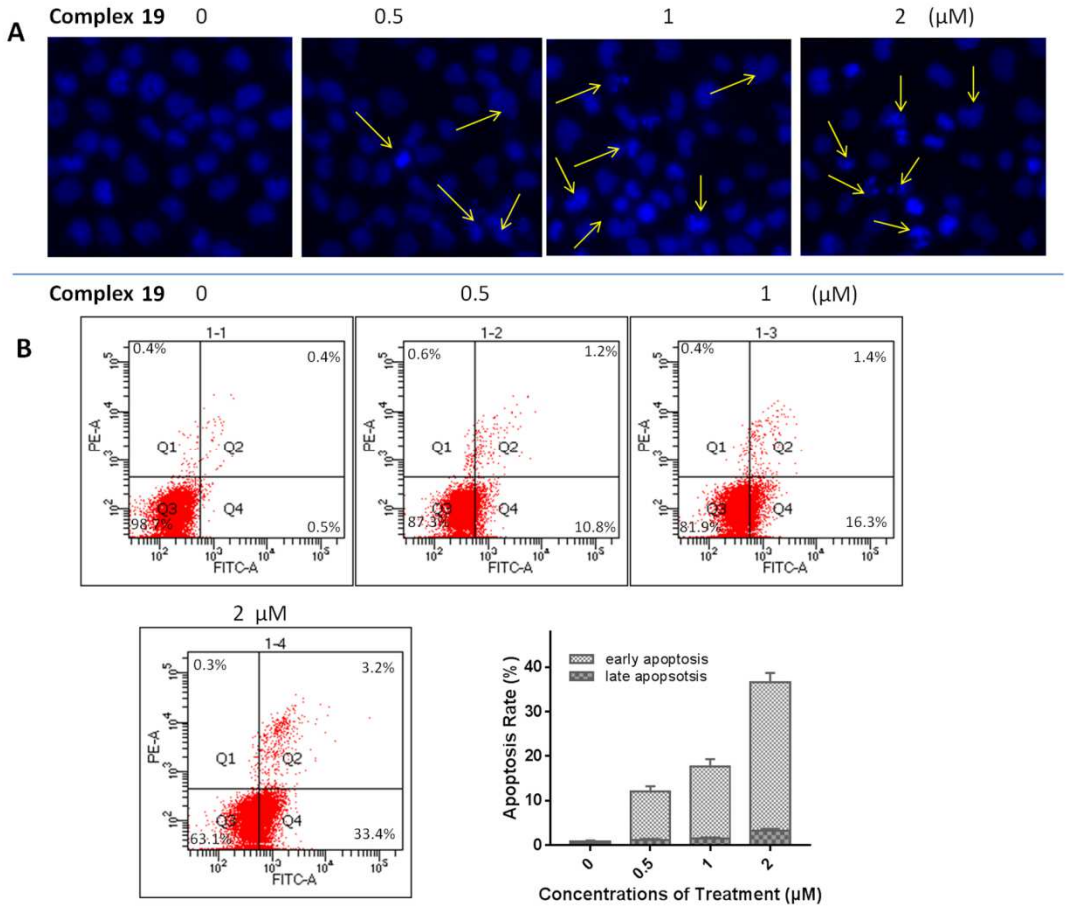

Fig. 4. Complex **19** induced apoptosis of MGC803 cells. (A) Apoptosis analysis with Hoechst 33258 staining; (B) Apoptosis of MGC803 cell line induced by complex **19** for 24 h using Annexin V-FITC/PI double staining and flow-cytometry calculation. The experiments were performed three times, and a representative experiment is shown.

To further investigate the underlying apoptotic mechanism of MGC803 cells induced by complex **19**, the western blot analysis was performed to investigate the expression change of apoptosis related proteins. As shown in Fig. 5A, it was observed that the expression of anti-apoptotic protein Bcl-2 decreased in a dose-dependent manner after treatment of MGC803 cells with complex **19** (Fig. 5B), while the expression of pro-apoptotic protein Bax was elevated accordingly (Fig. 5C). Besides, the accumulation of Bax was involved in activating the caspases, subsequently promoting the release of cytochrome and other pro-apoptotic factors from the mitochodria [26, 27], so that the expressions of both caspase-3 and caspase-9 were also examined. As shown in Fig. 5D and 5E, caspase-3/-9 were both upregulated

evidently, indicating the apoptosis occurring via the caspase-mediated pathway. Additionally, poly ADP-ribose polymerase (PARP) involved in DNA repair and gene integrity monitoring, was an important substrate of caspase-3, and PARP cleavage was considered as a hallmark of cell apoptosis [28]. And it was found that the cleaved PARP was clearly upregulated concentration-dependently (Fig. 5F). Taken together, all these results demonstrated that complex **19** could induce the apoptosis of MGC803 cells possibly via the mediation of intrinsic apoptotic pathway.

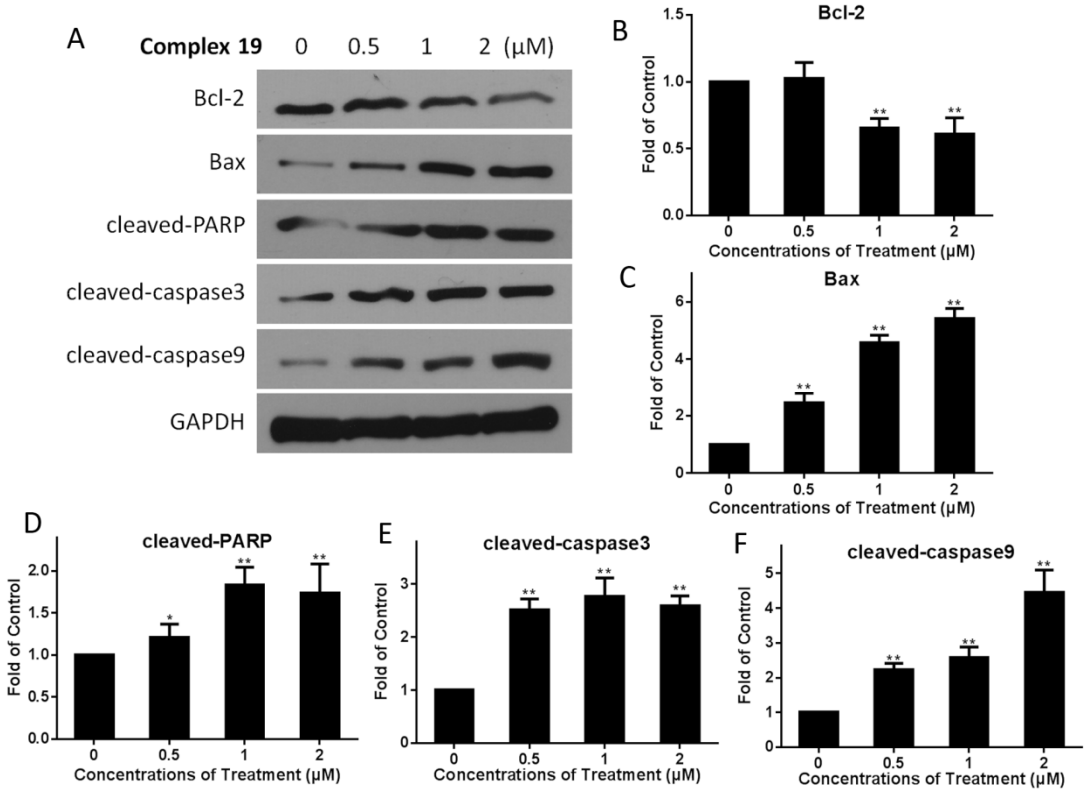

Fig. 5. Expression changes of apoptosis-related proteins induced by complex **19**. (A) Complex **19** induced expression changes of Bax, Bcl-2 and caspase family members in MGC803 cells; (B-F) Statistical analysis of expression levels of Bax, Bcl-2 and cleaved-caspased PARP/9/3.

3. Conclusions

In conclusion, the present study reveals a novel class of vanadium complexes as metal-based proliferative inhibitors. The antiproliferative results demonstrates that the synthetic vanadium complexes generally exerted moderate to good activities toward the tested cancer cell lines. Of note was that complex **19** exhibited the best as well as

wide-spectrum activity toward all the tested cancer cell lines, with the IC_{50} values ranging from 2.7 to 7.2 μM. In consideration of its good inhibition toward human gastric cancer cell line MGC803, complex **19** was further evaluated for its cellular activities, and the results indicated that complex **19** could remarkably inhibit the cell clonogenicity, migration, and EMT process of MGC803 cells. Also, complex **19** could induce the apoptosis of MGC803 via an innate apoptotic pathway. It was anticipated that complex **19** can serve as a template for developing new metallo agents for treatment of anticancer especially for gastric cancers.

4. Experimental section

4.1 General

All reagents and solvents were purchased from commercially available sources, and dry solvents were treated from an MBraun solvent purification system. The NMR spectra were recorded on Bruker-400 MHz for ^{1}H NMR, and 100 MHz for ^{13}C NMR spectrometer. Elemental analyses were recorded on an elemental Vario EL spectrometer. It should be noted that the targeted vanadium complexes were not characterized by NMR due to their paramagnetic nature of the vanadium center, but by the infrared spectra analysis.

4.2 General procedure for the synthesis of ligands and targeted complexes.

*4.2.1 The synthesis of intermediate **2a-h***

To a slurry of *t*BuOK (0.90 g, 1.5 eq) in 10 mL anhydrous diethyl ether was added 7-phenyl-1-indanone (1.0 g, 5 mmol, 1 eq) and 0.8 mL ethyl formate (2.0 eq) at 0 °C, and a large amount of white precipitate appeared immediately. The mixture was kept stirring at 0°C for 30 min, followed by warming to room temperature and stirred overnight. The reaction mixture was acidified with Formic acid in ethanol to adjust pH < 7, and the resultant solution was directly used for the next step without further purification to react with amine derivatives for preparation of imine ligands.

*4.2.2 The synthesis of ligand **4a** and complex **14***

Ligand **4a:** A Schlenk flask was charged with CuCl (4.8 mg, 0.048 mmol),

2-iodoaniline (0.12 mL, 1.05 mmol), trans-1,2-diaminocyclo- hexane (0.26 mL, 2.21 mmol), water (6.3 mL) and thiophenol (0.06 mL, 0.57 mmol). The flask was sealed under a positive pressure of argon and the resulting violet solution was heated overnight at 120^{o}C. The product was extracted from the aqueous layer with dichloromethane, dried and concentrated in vacuo. The crude mixture was then purified by flash chromatography (10 % CH_2Cl_2 in hexane) to give 2-(phenylthio)aniline **3** (102.1 mg, 97 %) as a colorless liquid. Then, the obtained **3** (1 eq) was added in the solution of **2a**, and the resultant reaction mixture was stirred over 24h at room temperature. Ligand **4a** was obtained by filtration without further purification, ^{1}H NMR (400 MHz, $CDCl_3$): δ 11.93, 8.04 (d, J_{HH} = 11.8, 13.5 Hz, 1H, O*H*), 7.85, 7.82 (d, J_{HH} = 11.8, 13.5 Hz, 1H, Ar-*H*), 7.61 (dd, J_{HH} = 7.6, 1.4 Hz, 1H, Ar-*H*), 7.56 (dd, J_{HH} = 7.7, 1.5 Hz, 1H, Ar-*H*), 7.53–7.42 (m, 4H, Ar-*H*), 7.41–7.32 (m, 3H, Ar-*H*), 7.29–7.19 (m, 3H, Ar-*H*), 7.19–7.10 (m, 2H, Ar-*H*), 7.02 (dtd, J_{HH} = 18.8, 7.6, 1.1 Hz, 1H, N=C*H*), 3.65, 3.41 (s, 2H, CH_2); ^{13}C NMR (100 MHz, $CDCl_3$) δ 193.28 (*C*-OH), 148.73 (N=*C*H), 146.95 (N-Ar), 141.24, 140.60 (S-Ar), 140.20, 137.48, 137.17, 136.38, 135.89, 135.38, 131.61, 130.47, 129.39, 129.24, 128.98, 127.27, 127.06, 126.42, 125.82, 125.68, 123.42, 123.12, 122.75, 121.16, 118.52, 113.58, 112.97, 112.74 (Ar), 109.60 (N=CH-*C*), 28.42 (*C*H_2); Anal. Calcd. for $C_{22}H_{19}ONS$: C, 76.49; H, 5.54; N, 4.05; S, 9.28. Found: C, 76.51; H, 5.53; N, 4.05; S, 9.26.

Complex **14**: To a suspension of NaH (60%, 1.2 eq) in dried THF was added ligand **4a** (1eq), and the resultant mixture was kept stirring over 4 h at room temperature, which was then added dropwise to a solution of $VCl_3(THF)_3$ (1.2 eq) in dried THF over 30 min. The reaction was stirred for another 16 h at room temperature, and treated by filtration to remove sodium chloride. The filtrate was concentrated in cacuo, followed by recrystallization in THF/hexane (v/v = 1/3) to give the desired complex **14**. FT-IR (KBr pellets): ν/cm^{-1} 3056, 2973, 2874, 1638, 1591, 1561, 1529, 1467, 1446, 1401, 1296, 1271, 1198, 1184, 1166, 1147, 1093, 1024, 1013, 967, 944, 918, 864, 755, 733, 689, 577, 540, 519, 493, 464, 446; Anal. Calcd. for $C_{26}H_{24}NO_2SVCl_2$: C, 58.22; H, 4.51; N, 2.61; S, 5.98. Found: C, 58.21; H, 4.51; N, 2.62; S, 5.95.

Similar experimental procedures were adapted for the preparation of list of complexes shown in Scheme 1.

*4.2.3 The synthesis of ligand **4b** and complex **15***

Ligand **4b**: ^{1}H NMR (400 MHz, $CDCl_3$): δ 11.77, 7.95 (d, J_{HH} = 11.6, 13.5 Hz, 1H, O*H*), 7.63-7.32 (m, 9H, Ar-*H*), 7.31-7.23 (m, 5H, Ar-*H*), 7.22-7.10 (m, 3H, Ar-*H*), 7.00 (dtd, J_{HH} = 16.3, 7.5, 1.2 Hz, 1H, N=C*H*), 3.66, 3.44 (s, 2H, CH_2); ^{13}C NMR (100 MHz, $CDCl_3$) δ 191.53 (*C*-OH), 148.95 (N=*C*H), 147.29 (N-Ar), 141.36, 141.00 (S-Ar), 140.27, 139.90, 137.52, 137.40, 136.46, 136.14, 135.15, 131.49, 130.69, 129.39, 128.57, 128.37, 127.70, 126.46, 126.40, 126.26, 125.37, 123.66, 121.46, 120.37, 112.42 (Ar), 108.65 (N=CH-*C*), 29.30 (*C*H_2); Anal. Calcd. for $C_{28}H_{21}ONS$: C, 80.16; H, 5.05; N, 3.34; S, 7.64. Found: C, 80.13; H, 5.03; N, 3.35; S, 7.66.

Complex **15**: FT-IR (KBr pellets): *v* 3078, 3052, 3035, 2970, 2885, 1594, 1561, 1489, 1469, 1442, 1425, 1393, 1297, 1277, 1259, 1197, 1165, 1089, 1076, 1036, 1016, 960, 924, 897, 859, 799, 788, 759, 743, 698, 591, 553, 526, 506, 491, 466, 453, 433 cm^{-1}; Anal. Calcd. for $C_{32}H_{28}NO_2SVCl_2$: C, 62.75; H, 4.61; N, 2.29; S, 5.24. Found: C, 62.77; H, 4.58; N, 2.29; S, 5.28.

*4.2.4 The synthesis of ligand **4c** and complex **16***

Ligand **4c:** To a Schlenk flask with positive pressure of argon was charged with CuCl (4.8 mg, 0.048 mmol), 2-iodoaniline (0.12 mL, 1.05 mmol), trans-1,2-diaminocyclo-hexane (0.26 mL, 2.21 mmol), 6.3 mL water and thiophenol (0.06 mL, 0.57 mmol) and the resultant mixture was brought to 120 ^{o}C and stirred overnight. The reaction misture was treated by extraction with DCM for three times, and then the organic phase was dried and concentrated in vacuo. The crude product was then subjected to flash chromatography (10 % CH_2Cl_2 in hexane) to give 2-(phenylthio)aniline **3** (102 mg, 97 %) as a colorless liquid [19]. Then, compound **3** (1 eq) was added in the solution of **2c**, and the reaction was stirred over 24 h at rt. Compound **4c** was readily obtained by filtration, ^{1}H NMR (400 MHz, $CDCl_3$): δ 11.77, 7.95 (d, J_{HH} = 11.7, 13.5 Hz, 1H, O*H*), 7.63-7.07 (m, 15H, Ar-*H*), 7.06-6.95 (m, 1H, N=C*H*), 3.65, 3.43 (s, 2H, CH_2), 2.40, 2.37 (s, 6H, C$\underline{H}_3$); ^{13}C NMR (100 MHz, $CDCl_3$)

δ 192.60 (*C*-OH), 149.98 (N=*C*H), 148.24 (N-Ar), 142.64, 142.10 (S-Ar), 141.66, 141.29, 138.49, 137.52, 137.29, 136.76, 136.05, 135.86, 132.43, 131.66, 130.49, 129.62, 129.43, 128.82, 127.67, 127.30, 126.43, 124.53, 122.46, 121.42, 113.51 (Ar), 109.79 (N=CH-*C*), 30.37 (*C*H_2), 21.48, 21.44 (*C*H_3); Anal. Calcd. for $C_{30}H_{25}ONS$: C, 80.50; H, 5.63; N, 3.13; S, 7.16. Found: C, 80.52; H, 5.62; N, 3.12; S, 7.14.

Complex **16**: FT-IR (KBr pellets): *v* 3054, 2962, 2910, 2886, 1595, 1561, 1476, 1447, 1405, 1389, 1286, 1271, 1192, 1159, 1110, 1067, 1036, 1018, 967, 926, 866, 857, 815, 788, 750, 692, 605, 580, 558, 537, 524, 490, 461, 450, 419 cm^{-1}; Anal. Calcd. for $C_{34}H_{32}NO_2SVCl_2$: C, 63.75; H, 5.04; N, 2.19; S, 5.01. Found: C, 63.77; H, 5.00; N, 2.18; S, 5.04.

*4.2.5 The synthesis of ligand **4d** and complex **17***

Ligand **4d**: ^{1}H NMR (400 MHz, $CDCl_3$): δ 11.87, 7.95 (d, J_{HH} = 11.8, 13.4 Hz, 1H, O*H*), 7.63-7.08 (m, 12H, Ar-*H*), 7.00 (dtd, J_{HH} = 8.7, 7.5, 1.2 Hz, 1H, N=C*H*), 6.73, 6.63 (d, J_{HH} = 2.3, 2.3Hz, 2H, Ar-*H*), 6.53, 6.50 (t, J_{HH} = 2.3, 2.3Hz, 1H, Ar-*H*), 3.81 (d, J_{HH} = 1.4Hz, 6H, C*H*$_3$), 3.65, 3.43 (s, 2H, C*H*$_2$); ^{13}C NMR (100 MHz, $CDCl_3$) δ 192.41 (*C*-OH), 150.09 (N=*C*H), 148.29 (N-Ar), 142.58, 142.01 (S-Ar), 141.15, 140.77, 140.40, 137.34, 136.54, 136.19, 135.83, 135.48, 132.47, 131.97. 131.72, 130.51, 129.47, 129.16, 128.89, 127.31, 126.38, 124.92, 122.55, 121.30, 113.38 (Ar), 108.24 (N=CH-*C*), 55.44 (O*C*H$_3$), 30.35 (*C*H_2); Anal. Calcd. for $C_{30}H_{25}O_3NS$: C, 75.13; H, 5.25; N, 2.92; S, 6.69. Found: C, 75.15; H, 5.26; N, 2.93; S, 6.67.

Complex **17**: FT-IR (KBr pellets): *v* 3058, 2961, 2879, 2837, 164, 1595, 1563, 1446, 1417, 1283, 1268, 1206, 1156, 1061, 1047, 1021, 999, 967, 927, 868, 814, 792, 748, 690, 603, 578, 556, 545, 494, 450 cm^{-1}; Anal. Calcd. for $C_{34}H_{32}NO_4SVCl_2$: C, 60.72; H, 4.80; N, 2.08; S, 4.77. Found: C, 60.73; H, 4.76; N, 2.09; S, 4.78.

*4.2.6 The synthesis of ligand **4e** and complex **18***

Ligand **4e**: ^{1}H NMR (400 MHz, $CDCl_3$): δ 11.79 (d, J_{HH} = 12.0 Hz, 1H, O*H*), 8.06-7.86 (m, 3H, Ar-*H*), 7.67-7.50 (m, 3H, Ar-*H*), 7.49-7.34 (m, 2H, Ar-*H*), 7.32-7.07 (m, 7H, Ar-*H*),7.03 (dtd, J_{HH} = 11.0, 7.5, 1.2 Hz, 1H, N=C*H*), 3.68, 3.46 (s, 2H, C*H*$_2$); ^{13}C NMR (100 MHz, $CDCl_3$) δ 191.89 (*C*-OH), 150.26 (N=*C*H), 148.56

(N-Ar), 142.29, 141.75 (S-Ar), 140.32, 137.71, 137.52, 137.38, 136.90, 136.48, 135.61, 132.78, 132.57, 132.01, 131.67, 130.68 (Ar), 130.41 (*C*F_3), 129.44, 129.32, 128.96, 128.83, 127.30, 126.34, 126.19, 122.88, 113.35 (Ar), 109.24 (N=CH-*C*), 30.42 (*C*H_2); ^{19}F NMR (376 MHz, $CDCl_3$): δ -62.56, -62.64 (s, 6F, C*F*$_3$); Anal. Calcd. for $C_{30}H_{19}ONSF_6$: C, 64.86; H, 3.45; N, 2.52; S, 5.77. Found: C, 64.85; H, 3.47; N, 2.54; S, 5.76.

Complex **18**: FT-IR (KBr pellets): *v* 3062, 2977, 2906, 2886, 1661, 1597, 1561, 1496, 1445, 1404, 1380, 1277, 1183, 1139, 1107, 1092, 1022, 984, 944, 899, 867, 808, 787, 750, 736, 710, 692, 681, 605, 583, 554, 532, 492, 449, 412 cm^{-1}; Anal. Calcd. for $C_{34}H_{26}NO_2SF_6VCl_2$: C, 54.56; H, 3.50; N, 1.87; S, 4.28. Found: C, 54.56; H, 3.48; N, 1.88; S, 4.31.

*4.2.7 The synthesis of ligand **4g** and complex **19***

Ligand **4g**: ^{1}H NMR (400 MHz, $CDCl_3$): δ 12.00, 8.05 (d, J_{HH} = 11.8, 13.6 Hz, 1H, O*H*), 7.60-7.56 (m, 1H, Ar-*H*), 7.47-7.29 (m, 7H, Ar-*H*), 7.25-7.05 (m, 9H, Ar-*H*), 7.01-6.93 (m, 1H, N=C*H*), 2.93-2.86 (m, 2H, C*H*$_2$), 2.66-2.60 (m, 2H, C*H*$_2$); ^{13}C NMR (100 MHz, $CDCl_3$) δ 186.75 (*C*-OH), 142.50 (N=*C*H), 142.47, 142.34 (S-Ar), 141.92 (N-Ar), 137.84, 136.51, 134.46, 132.45, 129.53, 129.50, 129.41, 128.62, 128.30, 127.73, 127.59, 127.11, 126.54, 126.12, 125.28, 125.13, 121.22, 120.43, 112.77 (Ar), 107.09 (N=CH-*C*), 30.20, 27.34 (*C*H_2); Anal. Calcd. for $C_{29}H_{23}ONS$: C, 80.34; H, 5.35; N, 3.23; S, 7.40. Found: C, 80.37; H, 5.37; N, 3.21; S, 7.39.

Complex **19**: FT-IR (KBr pellets): *v* 3056, 2946, 2094, 2879, 1644, 1583, 1550, 1481, 1463, 1445, 1416, 1380, 1329, 1281, 1267, 1231, 1212, 1180, 1154, 1092, 1071, 1027, 1016, 998, 951, 871, 856, 831, 802, 783, 758, 747, 732, 718, 696, 685, 649, 587, 554, 514, 467, 449 cm^{-1}; Anal. Calcd. for $C_{33}H_{30}NO_2SVCl_2$: C, 63.26; H, 4.83; N, 2.24; S, 5.12. Found: C, 63.28; H, 4.81; N, 2.22, S, 5.07.

*4.2.8 The synthesis of ligand **4h** and complex **20***

Ligand **4h**: ^{1}H NMR (400 MHz, $CDCl_3$): δ 12.07, 8.10 (d, J_{HH} = 11.2, 13.8 Hz, 1H, O*H*), 7.57 (dd, J_{HH} = 25.2, 7.6 Hz, 1H, Ar-*H*), 7.44-7.05 (m, 16H, Ar-*H*), 6.98 (m, 1H, N=C*H*), 2.70-2.62 (m, 2H, C*H*$_2$), 2.50-2.19 (m, 2H, C*H*$_2$), 1.87, 1.63 (t, J_{HH} = 6.6 Hz,

2H, CH_2); ^{13}C NMR (100 MHz, $CDCl_3$) δ 197.44 (*C*-OH), 142.81 (N=*C*H), 141.49, 140.88, 139.90, 139.64, 138.31, 137.10, 135.61, 130.41, 129.61, 129.52, 129.12, 128.87, 128.02, 127.28, 126.62, 126.40, 122.77, 121.98, 114.15, 110.29 (Ar), 30.85, 29.86, 27.95 (*C*H_2); Anal. Calcd. for $C_{30}H_{25}ONS$: C, 80.50; H, 5.63; N, 3.13; S, 7.16. Found: C, 80.47; H, 5.61; N, 3.11; S, 7.19.

Complex **20**: FT-IR (KBr pellets): *v* 3058, 2932, 2857, 1639, 1579, 1552, 1478, 1463, 1445, 1425, 1369, 1340, 1303, 1270, 1241, 1223, 1209, 1276, 1154, 1092, 1063, 1041, 1023, 1005, 991, 954, 918, 867, 852, 812, 783, 762, 751, 703, 689, 638, 605, 551, 533, 511, 456 cm^{-1}; Anal. Calcd. for $C_{34}H_{32}NO_2SVCl_2$: C, 63.75; H, 5.04; N, 2.19; S, 5.01. Found: C, 63.77; H, 5.01; N, 2.18; S, 5.03.

*4.2.9 The synthesis of ligand **4i** and complex **21***

Ligand **4i**: ^{1}H NMR (400 MHz, $CDCl_3$): δ 12.47, 8.10 (d, J_{HH} = 12.2, 14.0 Hz, 1H, O*H*), 7.46 (dd, J_{HH} = 7.6, 1.5 Hz, 1H, Ar-*H*), 7.43-7.29 (m, 6H, Ar-*H*), 7.28-7.14 (m, 5H, Ar-*H*), 6.90 (m, 1H, N=C*H*), 3.02, 2.94 (t, J_{HH} = 6.6 Hz, 2H, CH_2), 2.79, 2.70 (t, J_{HH} = 6.6 Hz, 2H, CH_2); 1.31, 1.15 (s, 9H, C(CH_3)$_3$); ^{13}C NMR (100 MHz, $CDCl_3$) δ 187.77 (*C*-OH), 144.58 (N=*C*H), 143.52 (N-Ar), 143.41 (S-Ar), 140.07, 138.22, 130.60, 130.45, 130.21, 128.66, 127.67, 127.06, 126.07, 121.44, 120.31, 112.07 (Ar), 107.72 (N=CH-*C*), 48.22 (S-*C*-(CH$_3$)$_3$), 31.17 (*C*H_2), 30.64 (C-(*C*H$_3$)$_3$), 28.30 (*C*H_2); Anal. Calcd. for $C_{27}H_{27}ONS$: C, 78.41; H, 6.58; N, 3.39; S, 7.75. Found: C, 78.42; H, 6.56; N, 3.41; S, 7.70.

Complex **21**: FT-IR (KBr pellets): *v* 3053, 2965, 2943, 2896, 2877, 2863, 2841, 1641, 1585, 1549, 1458, 1447, 1432, 1414, 1378, 1367, 1327, 1298, 1283, 1229, 1215, 1187, 1164, 1091, 1036, 1015, 946, 861, 804, 775, 760, 717, 702, 651, 629, 586, 553, 520, 484, 462, 448, 422 cm^{-1}; Anal. Calcd. for $C_{31}H_{34}NO_2SVCl_2$: C, 61.39; H, 5.65; N, 2.31; S, 5.29. Found: C, 61.37; H, 5.68; N, 2.33; S, 5.32.

*4.2.10 The synthesis of ligand **6** and complex **22***

Ligand **6**: ^{1}H NMR (400 MHz, $CDCl_3$): δ 11.68, 8.11 (d, J_{HH} = 9.8, 13.9 Hz, 1H, O*H*), 7.55-6.99 (m, 17H, Ar-*H*), 6.99-6.80 (m, 1H, N=C*H*), 3.69; 3.01-2.82; 2.71-2.58;1.21 (q, J_{HH} = 7.0 Hz; m; m; t, J_{HH} = 7.0 Hz; 4H, CH_2); ^{13}C NMR (100 MHz,

$CDCl_3$) δ 187.89 (*C*-OH), 145.03 (N=*C*H), 144.81 (N-Ar), 143.58 (S-Ar), 143.33, 143.21, 139.97, 134.57, 133.66, 133.32, 132.55, 130.70, 130.50, 130.43, 130.06, 129.58, 128.58, 128.28, 127.74, 127.27, 127.15, 126.52, 126.21, 124.66, 123.97, 123.01, 122.48, 122.02, 120.62, 118.67, 118.56, 117.78, 114.93, 113.83, 111.43 (Ar), 107.58 (N=CH-*C*), 31.28, 29.41, 28.23, 22.58 (*C*H_2); Anal. Calcd. for $C_{29}H_{23}O_2N$: C, 83.43; H, 5.55; N, 3.35. Found: C, 83.41; H, 5.56; N, 3.37.

Complex **22**: FT-IR (KBr pellets): *v* 3061, 2978, 2905, 1595, 1578, 1552, 1485, 1462, 1451, 1440, 1413, 1370, 1354, 1331, 1299, 1279, 1248, 1228, 1209, 1191, 1177, 1162, 1104, 1089, 1067, 1042, 1020, 1009, 944, 922, 878, 868, 849, 831, 813, 798, 780, 758, 748, 726, 708, 697, 660, 624, 588, 540, 508, 493, 479, 460, 439, 410 cm^{-1}; Anal. Calcd. for $C_{33}H_{30}NO_3VCl_2$: C, 64.93; H, 4.95; N, 2.29. Found: C, 64.95; H, 4.92; N, 2.26.

*4.2.11 The synthesis of ligand **7b** and complex **23***

Ligand **7b**: ^{1}H NMR (400 MHz, $CDCl_3$): δ 11.45 (d, J_{HH} = 11.6 Hz,1H, O-*H*), 7.41-7.22 (m, 11H, Ar-*H*), 7.17 (d, J_{HH} = 7.5 Hz, 1H, Ar-*H*), 7.00 (d, J_{HH} = 7.8 Hz, 2H, Ar-*H*), 6.97 (d, J_{HH} = 7.4 Hz, 1H, N=C-*H*), 2.95 (m, 2H, CH_2), 2.68 (m, 2H, CH_2). ^{13}C NMR (100 MHz, $CDCl_3$): δ 188.01 (N=*C*H), 143.76 (C=*C*-OH), 143.17, 140.97, 133.63, 130.60, 129.53, 128.45, 127.24, 126.43, 122.70, 116.06 (-Ar), 106.76 (C=*C*-CH=N), 31.38, 28.25 (*C*H_2). Anal. Calcd. for $C_{23}H_{19}NO$: C, 84.89; H, 5.89; N, 4.30. Found: C, 84.92; H, 5.88; N, 4.31.

Complex **23**: FT-IR (KBr pellets): *v*/cm^{-1} 3054, 3033, 2973, 2952, 2932, 2906, 2876, 2850, 1638, 1579, 1555, 1496, 1465, 1441, 1413, 1368, 1351, 1326, 1302, 1281, 1243, 1219, 1205, 1174, 1150, 1070, 1028, 1011, 963, 917, 883, 855, 831, 803, 782, 758, 706, 671, 661, 619, 592, 564, 543, 526, 505, 484, 439, 408. Anal. Calcd. for $C_{31}H_{34}NO_3VCl_2$: C, 63.06; H, 5.80; N, 2.37. Found: C, 63.07; H, 5.74; N, 2.32.

*4.2.12 The synthesis of ligand **7c** and complex **25***

Ligand **7c**: ^{1}H NMR (400 MHz, $CDCl_3$): δ 11.39 (d, J_{HH} = 11.1 Hz, 1H, O*H*,), 7.42-7.23 (m, 8H, Ar-*H*), 7.19 (d, J_{HH} = 7.5 Hz, 1H, N=C*H*), 2.97 (m, 2H, CH_2), 2.66 (m, 2H, CH_2). ^{13}C NMR (100 MHz, $CDCl_3$): δ 189.57 (N=*C*H), 143.97 (C=*C*-OH),

143.67, 142.84, 141.55, 133.03, 131.26, 130.69, 128.48, 127.91, 127.35, 126.61 (Ar), 109.91 (C=*C*-CH=N), 31.02, 28.14 (*C*H_2). ^{19}F NMR (376 MHz, $CDCl_3$): δ -154.82 (2F, *m*-Ar-*F*), -162.58 (2F, *o*-Ar-*F*), -164.70 (1F, *p*-Ar-*F*). Anal. Calcd. for $C_{23}H_{14}F_5NO$: C, 66.51; H, 3.40; N, 3.37. Found: C, 66.53; H, 3.42; N, 3.37.

Complex **25**: FT-IR (KBr pellets): *v*/cm^{-1} 3058, 3034, 2973, 2955, 2927, 2911, 2867, 2838, 1589, 1557, 1464, 1446, 1433, 1363, 1334, 1297, 1263, 1235, 1225, 1194, 1179, 1166, 1153, 1110, 1093, 1058, 1037, 1013, 965, 933, 916, 877, 857, 829, 806, 784, 773, 758, 704, 678, 667, 648, 620, 600, 594, 577, 567, 549, 512, 503, 480, 460, 447, 423. Anal. Calcd. for $C_{31}H_{29}F_5NO_3VCl_2$: C, 54.72; H, 4.30; N, 2.06. Found: C, 54.71; H, 4.25; N, 2.08.

*4.2.13 The synthesis of ligand **10** and complex **26***

Ligand **10**: ^{1}H NMR (400 MHz, $CDCl_3$): δ 12.07-11.67 (m, 1H, O*H*), 7.56-7.06 (m, 22H, Ar-*H*), 6.97-6.82 (m, 1H, N=C*H*), 2.98-2.79; 2.67-2.53; 2.48-2.39 (m, 4H, CH_2); ^{13}C NMR (100 MHz, $CDCl_3$) δ 186.59 (*C*-OH), 143.41 (N=*C*H), 143.20 (N-Ar), 142.49 (S-Ar), 142.46, 142.40, 139.88, 134.19, 134.01, 133.92, 133.40, 133.20, 132.88, 132.72, 132.52, 132.50, 130.01, 129.56, 129.40, 129.34, 128.98, 128.29, 127.89, 127.81, 127.66, 127.43, 127.36, 127.18, 126.63, 126.54, 126.05, 125.93, 125.41, 125.08, 121.74, 114.17, 114.15 (Ar), 100.52 (N=CH-*C*), 30.24, 28.31, 27.16, 21.39 (*C*H_2); ^{31}P (162 MHz, $CDCl_3$) δ -19.98, -22.52; Anal. Calcd. for $C_{35}H_{28}ONP$: C, 82.49; H, 5.54; N, 2.75. Found: C, 82.51; H, 5.59; N, 2.76.

Complex **26**: FT-IR (KBr pellets): *v* 3056, 3025, 2952, 2879, 1584, 1550, 1481, 1462, 1451, 1438, 1417, 1378, 1350, 1312, 1295, 1280, 1252, 1230, 1215, 1181, 1159, 1123, 1091, 1065, 1027, 1016, 1001, 956, 868, 857, 829, 803, 784, 772, 754, 745, 735, 716, 699, 694, 670, 651, 621, 591, 574, 563, 546, 521, 507, 495, 482, 452, 433, 418 cm^{-1}; Anal. Calcd. for $C_{39}H_{35}NO_2PVCl_2$: C, 66.68; H, 5.02; N, 1.99. Found: C, 63.67; H, 5.05; N, 1.99.

*4.2.14 The synthesis of ligand **12** and complex **27***

Ligand **12**: ^{1}H NMR (400 MHz, $CDCl_3$): δ 10.81, 8.24 (d, J_{HH} = 13.1, 13.2 Hz, 1H, O*H*), 7.71-7.54 (m, 6H, Ar-*H*), 7.54-7.19 (m, 15H, Ar-*H*), 7.15 (d, 1H, J_{HH} = 7.4 Hz,

Ar-*H*), 6.98; 6.88 (dd, J_{HH} = 13.7, 7.6 Hz; t, J_{HH} = 6.8 Hz; 1H, N=C*H*), 3.74; 3.01-2.88; 2.88-2.74;1.85 (s; m; m; t, J_{HH} = 6.3 Hz; 4H, CH_2); ^{13}C NMR (100 MHz, $CDCl_3$) δ 186.04 (*C*-OH), 147.08 (N=*C*H), 144.01 (N-Ar), 143.54 (S-Ar), 143.36, 136.20, 133.91, 133.44, 133.34, 132.73, 132.52, 132.50, 132.07, 131.97, 131.06, 130.74, 130.33, 128.82, 128.70, 128.21, 127.67, 127.62, 126.43, 120.81, 120.68, 115.28, 114.98, 114.91, 114.27 (Ar), 112.53 (N=CH-*C*), 67.96, 29.43, 25.60, 22.72 (*C*H_2); ^{31}P (162 MHz, $CDCl_3$) δ 37.46, 37.13; Anal. Calcd. for $C_{35}H_{28}O_2NP$: C, 79.98; H, 5.37; N, 2.67. Found: C, 80.01; H, 5.39; N, 2.66.

Complex **27**: FT-IR (KBr pellets): *v* 3056, 3020, 2950, 2900, 1637, 1586, 1557, 1480, 1462, 1451, 1440, 1415, 1371, 1349, 1328, 1298, 1280, 1251, 1226, 1211, 1193, 1175, 1160, 1120, 1088, 1059, 1037, 1026, 1015, 997, 953, 920, 866, 859, 833, 804, 782, 757, 728, 717, 695, 670, 655, 690, 571, 561, 550, 528, 521, 510, 488, 473, 448, 430 cm^{-1}; Anal. Calcd. for $C_{39}H_{35}NO_3PVCl_2$: C, 65.19; H, 4.91; N, 1.95. Found: C, 65.17; H, 4.92; N, 1.93.

4.3 Antiproliferative activity assays

Exponentially growing cells were added into 96-well plates at a concentration of about 3,000 cells per well. Over a period of 24 h, the culture medium was discarded, and fresh medium containing indicated concentrations of tested compounds was added to each well. After 72 h incubation, 3-(4,5-dimethylthiazol-2-yl)-2,5-diphenyltetrazolium bromide (MTT) solution was added into each well and stood for another 4 h. Then the medium was removed, followed by the addition of 150 μL DMSO for each well. The plate was agitated on the plate shaker to make the dark blue crystal dissolved. And MTT assays were performed and cell viability was assessed at 570nm by a microplate reader (Biotech, Shanghai, China).

4.4 Clonogenicity assay

MGC803 cells (about 1000 cells/well) were seeded in a 6-well plate and incubated for 24 h, then the media were removed followed by adding the fresh media containing indicated concentrations of complex **19**. After 9 days of incubation, the cells were washed with PBS for three times, and then fixed with 4% paraformaldehyde for

30min. The cell colonies were then visualized by using 0.1% crystal violet staining. The cells were then imaged, and the colony populaton were quantified by Image J software (Developed by National Institutes of Health).

4.5 Hoechst 33258 staining

MGC803 cells were seeded in a 6-well plate (2×10^5/well), and incubated overnight for adherent followed by treatment with complex **19** at indicated concentrations for 24 h. Hoechst 33258 was used for cell staining over 30 min in the dark. The cells were observed under a Nikon Eclipse TE 2000-S fluorescence microscope (Nikon, Japan).

4.6 Transwell migration assay

100 mL medium containing 1% FBS, indicated concentrations of complex **19** with 10,000 MGC803 cells were added to each upper chambers of Transwell plate. Then 500 μL medium with 20% FBS was used as chemoattractant in the lower chambers. After 72 h of incubation, both chambers were washed with PBS for three times, followed by staining with Hoechst33258 (10 μg/mL) for 15 min. The migrated cells were determined by using high content screening system (ArrayScan XTI, Thermo Fisher Scientific).

4.7 Cell apoptosis assay

MGC803 cells were seeded into a 6-well plate (2×10^5/well) and incubated for 24 h. Then the cells were treated with indicated concentrations of the tested complex **19** for 24 h. Thereafter, the cells were collected and the Annexin-V-FITC/PI apoptosis kit (Biovision) was used according to the manufacturer's protocol. The cells were analyzed by high content screening system (ArrayScan XTI, Thermo Fisher Scientific, MA).

4.8 Western blot analysis

MGC803 cells were treated with different concentrations of complex **19** for 24 h, the cells were collected, lysed in radio-immunoprecipitation assay (RIPA) buffer contained protease inhibitor cocktail for 30 min, followed by centrifugation at 12,000

rpm for 10 min at 4 ^{o}C. After collecting the supernatant, the protein was determined using a bicinchonininc acid assay kit (Beyotmie Biotechnology, Haimen, China). Then cell lyses were boiled with loading buffer for 10 min at 100 ^{o}C for SDS-polyacrylamide gel electrophoresis (PAGE). Proteins were transferred to nitrocellulose (NC) membranes and then were blocked with 5% skim milk at room temperature for 2 h, followed by incubation with primary antibodies at 4^{o}C overnight. Next, the membrane was washed with the secondary antibody (1: 5000) at room temperature for 2 h. Finally, the blots were washed in TBST/TBS and the immunoblots were visualized by enhanced chemiluminescence (ECL) and exposed on Kodak radiographic film.

4.9 Statistical analysis

All experimental data in biology were expressed as means ± SD. Statistical significance between two groups was evaluated by the Student's t-test. P value less than 0.05 was considered statistically significant.

Acknowledgement

This work was supported by Zhengzhou University of Industrial Technology Natural Science Foundation (Project No.2018YB020) and Foundation of The Science and Technology Department of Henan Province (Project No. 182102310169).

References

[1] K.H. Thompson, C. Orvig, Coordination chemistry of vanadium in metallopharmaceutical candidate compounds, Coordin Chem Rev, 219-221 (2001) 1033-1053.

[2] D.C. Crans, J.J. Smee, E. Gaidamauskas, L. Yang, The chemistry and biochemistry of vanadium and the biological activities exerted by vanadium compounds, Chem Rev, 104 (2004) 849-902.

[3] D. Sanna, M. Serra, V. Ugone, L. Manca, M. Pirastru, P. Buglyo, L. Biro, G. Micera, E. Garribba, Biorelevant reactions of the potential anti-tumor agent vanadocene dichloride, Metallomics : integrated biometal science, 8 (2016) 532-541.

[4] D. Rehder, The potentiality of vanadium in medicinal applications, Future Med Chem, 4 (2012) 1823-1837.

[5] J.C. Pessoa, I. Tomaz, Transport of Therapeutic Vanadium and Ruthenium Complexes by Blood Plasma Components, Curr Med Chem, 17 (2010) 3701-3738.

[6] A. Sheela, S.M. Roopan, R. Vijayaraghavan, New diketone based vanadium complexes as insulin mimetics, Eur J Med Chem, 43 (2008) 2206-2210.

[7] Z. Kazemi, H. Amiri Rudbari, V. Mirkhani, M. Sahihi, M. Moghadam, S. Tangestaninejad, I. Mohammadpoor-Baltork, A.A. Kajani, G. Azimi, Self-recognition of the racemic ligand in the formation of homochiral dinuclear V(V) complex: In vitro anticancer activity, DNA and HSA interaction, Eur J Med Chem, 135 (2017) 230-240.

[8] C. Yang, F. Ma, J. Tang, L. Han, S. Wei, L. Zhou, J. Zhou, J. Shen, F. Wang, Synthesis of vanadyl-hypocrellin A complex and its photodynamic properties research, Bioorg Med Chem Lett, 22 (2012) 5003-5007.

[9] M.J. Xie, L. Li, X.D. Yang, W.P. Liu, S.P. Yan, Y.F. Niu, Z.H. Meng, A new insulin-enhancing agent: [N,N'-bis(4-hydroxysalicylidene)-o-phenylene-diamine]oxovanadium(IV) and its permeability and cytotoxicity, Eur J Med Chem, 45 (2010) 2327-2335.

[10] D.C. Crans, J.J. Smee, E. Gaidamauskas, L.Q. Yang, The chemistry and biochemistry of vanadium and the biological activities exerted by vanadium compounds, Chem Rev, 104 (2004) 849-902.

[11] Y. Jia, L. Lu, M. Zhu, C. Yuan, S. Xing, X. Fu, A dioxidovanadium (V) complex of NNO-donor Schiff base as a selective inhibitor of protein tyrosine phosphatase 1B: Synthesis, characterization, and biological activities, Eur J Med Chem, 128 (2017) 287-292.

[12] T.C. Ting, M.Y. Chang, T.Y. Hsu, W.P. Wang, Y.J. Hsieh, C.J. Chang, Vanadocene dichloride inhibits cell proliferation by targeting Aurora B, Metallomics : integrated biometal science, 10 (2018) 1099-1106.

[13] P. Ghosh, O.J. D'Cruz, R.K. Narla, F.M. Uckun, Apoptosis-inducing vanadocene compounds against human testicular cancer, Clinical cancer research : an official journal of the American Association for Cancer Res, 6 (2000) 1536-1545.

[14] R. Havelek, P. Siman, J. Cmielova, A. Stoklasova, J. Vavrova, J. Vinklarek, J. Knizek, M. Rezacova, Differences in vanadocene dichloride and cisplatin effect on MOLT-4 leukemia and human peripheral blood mononuclear cells, Med Chem, 8 (2012) 615-621.

[15] C.S. Navara, A. Benyumov, A. Vassilev, R.K. Narla, P. Ghosh, F.M. Uckun, Vanadocenes as potent anti-proliferative agents disrupting mitotic spindle formation in cancer cells, Anti-cancer drugs, 12 (2001) 369-376.

[16] X. Stachtea, N. Karamanos, N. Klouras, Enhanced antitumour activity of cyclopendadienyl-substituted metallocene dihalides in human breast and colon cancer cells, Anticancer Res, 29 (2009) 3227-3231.

[17] C. Datta, D. Das, P. Mondal, B. Chakraborty, M. Sengupta, C.R. Bhattacharjee, Novel water soluble neutral vanadium(IV)-antibiotic complex: Antioxidant, immunomodulatory and molecular docking studies, EurJ Chem Med, 97 (2015) 214-224.

[18] L.P. Lu, J.B. Wang, J.Y. Liu, Y.S. Li, Synthesis, structural characterization, and ethylene polymerization behavior of (arylimido)vanadium (V) complexes bearing tridentate shciff base ligands, Polym Sci., Part A: Polym Chem, 52 (2014) 2633-2642.

[19] M. Carril, R. SanMartin, E. Dominguez, I. Tellitu, Simple and efficient recyclable catalytic system for performing copper-catalysed S-arylation reactions in the presence of water, Chem-Eur J, 13 (2007) 5100-5105.

[20] C. Zhang, C. Li, J. Bai, H. Li, A Cu Nanoparticle Embedded in Electrospundoped Carbon Nanofibers as Efficient Catalysts for Ullmann O-Arylation of Aryl Halides with Various Phenols, Catal Lett, 145 (2015) 1764-1770.

[21] Y.C. Duan, Y.C. Ma, E. Zhang, X.J. Shi, M.M. Wang, X.W. Ye, H.M. Liu, Design and synthesis of novel 1,2,3-triazole-dithiocarbamate hybrids as potential anticancer agents, Eur J Med Chem, 62 (2013)

11-19.

[22] C. Wang, L. Jiang, S. Wang, H. Shi, J. Wang, R. Wang, Y. Li, Y. Dou, Y. Liu, G. Hou, Y. Ke, H. Liu, The Antitumor Activity of the Novel Compound Jesridonin on Human Esophageal Carcinoma Cells, PloS one, 10 (2015) e0130284.

[23] A.I. Elkady, O.A. Abuzinadah, N.A. Baeshen, T.R. Rahmy, Differential control of growth, apoptotic activity, and gene expression in human breast cancer cells by extracts derived from medicinal herbs Zingiber officinale, J Biomed Biotechnol, 2012 (2012) 614356.

[24] S. Elmore, Apoptosis: a review of programmed cell death, Toxicol pathol, 35 (2007) 495-516.

[25] R.S. Harapanhalli, R.W. Howell, D.V. Rao, Bis-benzimidazole dyes, Hoechst 33258 and Hoechst 33342: radioiodination, facile purification and subcellular distribution, Nucl Med Biol, 21 (1994) 641-647.

[26] X.J. Shi, B. Yu, J.W. Wang, P.P. Qi, K. Tang, X. Huang, H.M. Liu, Structurally novel steroidal spirooxindole by241 potently inhibits tumor growth mainly through ROS-mediated mechanisms, Sci Rep, 6 (2016) 31607.

[27] A. Didonna, J. Sussman, F. Benetti, G. Legname, The role of Bax and caspase-3 in doppel-induced apoptosis of cerebellar granule cells, Prion, 6 (2012) 309-316.

[28] M. Los, M. Mozoluk, D. Ferrari, A. Stepczynska, C. Stroh, A. Renz, Z. Herceg, Z.Q. Wang, K. Schulze-Osthoff, Activation and caspase-mediated inhibition of PARP: a molecular switch between fibroblast necrosis and apoptosis in death receptor signaling, Mol Biol Cell, 13 (2002) 978-988.

Highlights

- A library of vanadium complexes showed moderate to good growth inhibition against the tested cancer cells.
- Complex **19** demonstrated the best as well as selective proliferation inhibition toward MGC-803 cells.
- Complex **19** inhibited the cell colony formation, migration and EMT process of MGC803.
- Complex **19** induced the apoptosis of MGC-803 cells, and led to the expression changes of key proteins related to apoptosis.